JOURNAL OF AGRICULTURAL AND FOOD CHEMISTRY

Using Proteomics, Immunohistology, and Atomic Force Microscopy To Characterize Surface Damage to Lambskins Observed after Enzymatic Dewooling

RICHARD L. EDMONDS,[†] SANTANU DEB CHOUDHURY,[§] RICHARD G. HAVERKAMP,[#] MERVYN BIRTLES,[⊥] TIMOTHY F. ALLSOP,[†] AND GILLIAN E. NORRIS*,[§]

New Zealand Leather and Shoe Research Association, Palmerston North, New Zealand 4442; and Institute of Molecular Biosciences, Institute of Technology and Engineering, and Institute of Veterinary, Animal and Biomedical Sciences, Massey University, Palmerston North, New Zealand 4442

The effects of conventional lime sulfide depilation and enzymatic depilation on the enamel layer of pickled lamb pelts were examined using atomic force and optical microscopy, immunohistological, and proteomic techniques. Microscopy showed that the surface structure of enzymatically depilated material was visibly less organized than conventionally processed material, implying that the enzymes used for depilation were responsible for this difference. Proteomic analyses identified an absence of collagen VI in the enamel of skins that had been processed with enzymes, in contrast to the skins that had been processed using conventional methods, which was confirmed using immunolocalization studies. It is therefore possible that the destruction of collagen VI during enzymatic depilation may cause the changes to the enamel structure observed during enzyme processing and in turn affect the quality of the finished product.

KEYWORDS: Atomic force microscopy; peptide mass fingerprinting; MALDI-TOF mass spectrometry; leather; papillary layer; collagen VI

INTRODUCTION

Enzymatic depilation and processing of animal skins has been the focus of much research recently (*1–3*) because of the potential savings in both chemical and environmental costs plus the associated improvement in the workplace (*4, 5*). Conventional processing of lambskins to produce pickled pelts entails sequential treatment of the skin with a strong alkaline sulfide depilation to loosen wool followed by a prolonged exposure to alkaline conditions at around pH 12.5, which degrades any remaining wool and washes out alkali-soluble proteins (*6*). The epidermal keratin, which is responsible for the hydrophobic surface of the skin, is destroyed at this stage of the process (*7*). After washing, the pH of the skin is adjusted to about 8, the temperature is raised to 35 °C, and protease is added to break down and remove other noncollagenous proteins both from the interfibrillular matrix of the skin and from the upper (grain) surface to impart a smooth feel to the surface and improve its appearance (*8*). The skin is then washed repeatedly to remove any residual soluble materials before it is pickled in a salt and sulfuric acid solution at pH 1.0. In this form, it is relatively stable to putrefaction and is ready for tanning. This sequence of processes has a profound effect on the quality of the leather, as it results in the removal of most of the proteins and proteoglycans, except for the collagens (*9*) and elastin.

Sodium sulfide is unpleasant to work with, polluting, and potentially hazardous. Alternative processing regimens using enzymes have been investigated as they have the potential to overcome these problems. However, they will not be acceptable until it can be shown that the finished product is consistently the equal of that which has been conventionally processed. Although enzymes are currently used during conventional leather processing, the concentrations used are appreciably less than those required for complete dewooling and skin processing. In contrast, when proteolytic enzymes are used to dewool and process skins in the absence of sodium sulfide (a chemical depilatory), the pelt is inevitably damaged (*10*). Of particular concern is damage to the layer of the skin that becomes the outermost layer after processing. Comprising the uppermost surface of the dermis, this region is defined as the enamel layer and can be clearly distinguished from the rest of the dermis. It is about 100 μm thick and lies immediately below the cells of the epidermis at the top of the papillary layer of the dermis (*11*). Because it is the outer surface of the pickled pelt product, the enamel layer is responsible for the outward appearance of the final leather and is therefore the most valuable part of the

* Author to whom correspondence should be addressed (e-mail g.norris@massey.ac.nz).
[†] New Zealand Leather and Shoe Research Association.
[§] Institute of Molecular Biosciences, Massey University.
[#] Institute of Technology and Engineering, Massey University.
[⊥] Institute of Veterinary, Animal and Biomedical Sciences, Massey University.

10.1021/jf800380y CCC: $40.75
Published on Web 08/14/2008

pelt. If it is in good condition, the skin is worth significantly more in comparison to skins with a damaged enamel layer.

Previous work aimed at determining the nature of this surface has been limited mostly to optical and scanning electron microscopy (*11, 12*). These studies showed that the enamel has a different collagen morphology from that of the rest of the grain layer below it (*11, 13*). In particular, the distribution of the diameter of the fibrils in the enamel and the grain layers was shown to be significantly different (*14*).

Previous isoelectric focusing experiments have shown that proteins from pickled pelt focus in the pH range of 4−7 and that the protein complement of the raw skin is severely depleted after conventional processing (*9*). Because collagens are the major component of the pickled pelt, they dominate the sample in any type of analysis, making it difficult to detect differences in the minor components. To determine whether there are any differences in the populations of minor proteins between the enzymatic and conventionally depilated skins, these minor proteins need to be enriched. However, it is difficult to remove one component of a complex mixture of proteins without the loss of others. Another approach is to isolate the layer of the skin of interest, on the assumption that the specific proteins important for its integrity will be present in higher concentrations.

The present work focuses on the fine structure and composition of the enamel layer relative to that of the remainder of the grain layer. Our strategy was to characterize the nature of the grain enamel layer, to determine the differences in the protein complement of this layer from skins subjected to different processing regimes, and to determine the effect of the different regimens on the proteins in this layer.

MATERIALS AND METHODS

Reagents. Tris(hydroxymethyl)aminomethane, 3-[(3-cholamidopropyl)dimethylammonio]-1-propanesulfonate (CHAPS), thiourea, urea, iodoacetamide (IAM), sodium dodecyl sulfate (SDS), *N*-ethylmaleimide, α-cyano-4-hydroxy-*trans*-cinnamic acid, dithiothreitol (DTT), and diaminobenzidine were purchased from Sigma. pH 4−7 carrier ampholytes, biotinylated antibody raised against rabbit, and biotin−streptavadin−peroxidase complex were from Amersham Biosciences. Sequence-grade modified porcine trypsin was obtained from Promega. Phenylmethanesulfonyl fluoride (PMSF), *N*-(2-hydroxyethyl)piperazine-*N*′-(2-ethanesulfonic acid) (HEPES), sodium carbonate, sodium bicarbonate, and sodium dihydrogen orthophosphate were obtained from BDH Chemicals Ltd. (Poole, U.K.). Complete Mini was obtained from Roche Diagnostics, Mayers Hämalaun solution from Applichem GmbH, Darmstadt, Germany, DPX mounting medium from Labchem, Australia, and 30% peroxide solution from Scharlau Chemie, Spain. Acetonitrile, butanol, and dichloromethane were from SDS Chemicals (France). Rabbit anti-human collagen type VI polyclonal antibody was obtained from Chemicon International. The following commercial grade chemicals were also used: Tanzyme, a proprietary liquid extract of lamb pancreas containing both proteolytic and lipolytic enzymes (Tryptec Biochemicals, New Zealand); Purafect, a proprietary liquid alkaline protease from *Bacillus subtilis* (Zymus International Ltd.); ammonium sulfate (Clark Products, New Zealand), hydrated lime (Websters Hydrated Lime Co. Ltd., New Zealand), and starch thickener (Solvitose, Avebe, The Netherlands). All other chemicals were all of analytical grade.

Appropriate laboratory safety procedures were used while handling these chemicals.

Skin Preparation by Conventional Method. A cross-breed Romney skin was used for this experiment. After removal of the skin from the carcass, it was immediately cooled to 10 °C and then transported to the laboratory, where any adhering fat and flesh were mechanically removed prior to processing. The skin was divided lengthways into halves, one of which was conventionally processed and the other enzyme depilated.

Conventional lime sulfide paint comprising 140 g/L commercial flake sodium sulfide, 50 g/L hydrated lime, and 23 g/L pregelled starch thickener was applied to the flesh (inner) side of the "conventional" skin at a rate of 400 g/m^2. The skin was then incubated at 20 °C for 16 h, after which time the wool was manually removed. The skin was then processed in a drum with 0.8 volume of water for 6 h, after which it was washed with four changes of 2 volumes of water to remove the lime. One volume of 2% (w/v) ammonium sulfate was then added, which lowered the pH to about 8, followed by the addition of 0.1% (w/v) Tanzyme, a commercial bate enzyme, in water. After a period of 75 min at 35 °C, the treated skin was washed with four changes of 2 volumes of cold water (20 °C) and then pickled by the addition of 1 volume of pickle solution (20% w/v common salt and 2% w/v sulfuric acid diluted in water). The pickled skin material was thus preserved from bacterial decomposition.

Skin Preparation by Enzymatic Method. The other half of the skin was soaked for 30 min in 0.5 M sodium carbonate/bicarbonate buffer at pH 10.5 containing 4% (v/v) Purafect, an industrial protease. After incubation for 30 min, excess enzyme solution was removed from the skin pieces by centrifugation. The skin was then held overnight (20 h) at 20 °C, after which time the wool was removed through the application of pressure to the wool roots by drawing a thumb across the skin. The amount of pressure applied was increased until dewooling occurred or until grain cracking could be observed, at which point dewooling was discontinued. Once dewooling was complete, the skin was pickled using the procedure described above.

Skin Sectioning for Optical Microscopy AFM and Electrophoretic Studies. Square pieces of skin approximately 5 × 5 mm were excised from equivalent areas of the differently processed half-skins and placed flat on a cryostat stub. Frozen samples of skin 20 μm thick were cut horizontally from the upper (grain) surface with a cryostat (Jung Frigocut 2800E, Leica) and examined under a binocular Nikon Optishot microscope at 50× magnification. The sections were designated as being either the grain enamel layer or the remaining grain layer according to their appearance. The first four 20 μm sections cut from the upper surface of each sample were designated "enamel". The next six sections contained significant amounts of both the enamel and the remaining grain layers as illustrated in **Figure 1** and so were discarded, and the following six sections were collected and designated "remaining grain layer". These samples were then prepared for 2D electrophoresis. A second set of excised skin samples was prepared, and the uppermost section of the enamel layer was fixed to a slide and examined using atomic force microscopy.

Extraction of Proteins for Electrophoretic Studies. The skin sections were cut into small pieces, immersed in liquid nitrogen, and then ground using a mortar and pestle; the resulting powder was stored at −80 °C for further use. The powdered samples were then suspended in 5 volumes of lysis solution, containing 8 M urea, 2 M thiourea, 4% CHAPS, 20 mM DTT, and Complete Mini (wide-spectrum protease inhibitor at the concentration recommended by the manufacturer) in 40 mM Tris buffer (pH 7.0) for 1 h at room temperature. After this time, they were briefly sonicated (Cole-Palmer, model 8891), taking care not to heat the samples, and then centrifuged for 15 min at 7500*g* to remove any insoluble material, and the supernatant was collected and stored at −80 °C for further studies (*15*).

Prior to determination of their protein concentrations, the samples were dialyzed against Tris-HCl buffer (pH 7.0) to remove any chaotropic agents and detergents that might interfere with the Bradford reagent. Protein concentrations were then determined using the Bradford method, with BSA as the standard (*16*).

Atomic Force Microscopy Studies. An atomic force microscope (MFP-3D Asylum Research, Santa Barbara, CA) was used to study the differences in the surface topology of skins treated using conventional methods or enzymes. Silicon cantilevers (Ultrasharp CSG-11, NT-MDT, Zelenograd, Moscow, Russia) were used to study the samples in contact mode. The tip, nominally 10 nm in radius, was located on the free end of a cantilever 350 μm long, 35 μm wide, and 0.7−1.3 μm thick with a nominal force constant of 0.01−0.08 N/m. A tip speed of 40 μm/s was used to scan the samples.

2D Gel Electrophoresis. Isoelectric focusing was carried out at 20 °C using an IPGphor unit (Amersham Biosciences). Pickled skin

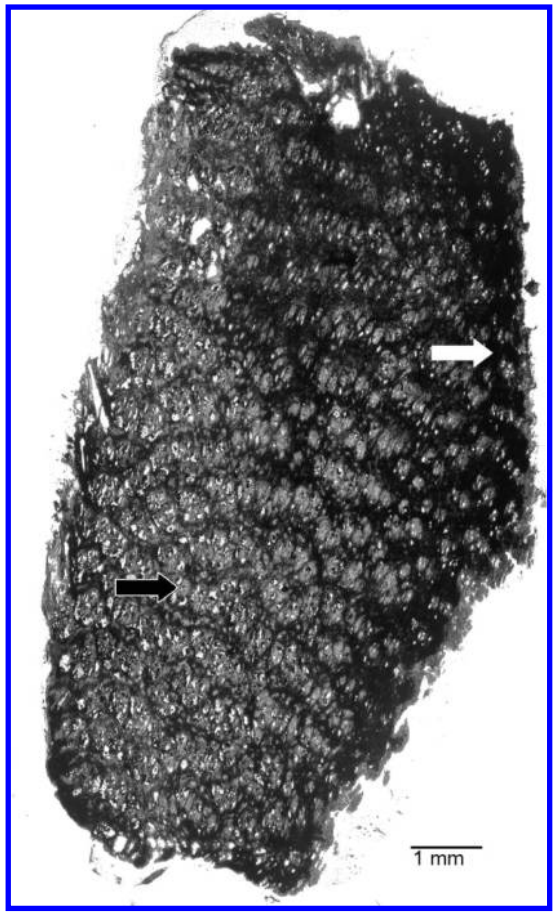

Figure 1. Section of conventional skin. Twenty micrometer sections were cut from the surface of the skin to prepare samples for this work. This image represents the sixth section cut from the surface of conventionally processed skin, which contains regions of both the enamel layer and the remainder of the grain layer. The enamel layer is visible as the darker region (white arrow) around the outside of the section, particularly at the top right of the image. The lighter region (black arrow) is the remainder of the grain layer that has been uncovered by the removal of successive sections.

extracts (50 uL) having total protein concentrations of approximately 0.1 mg/mL were solubilized by incubation for 30 min in 125 μL of rehydration solution (2 M thiourea, 8 M urea, 20 mM DTT, 0.5% v/v IPG buffer, pH 4−7, a trace of bromophenol blue, 2% CHAPS, and Complete Mini). The solution was then centrifuged at 11300*g* for 2 min, and the clear supernatant was applied to 7 cm IPG strips (Amersham Biosciences), pH 3−10. The process was repeated for the longer IPG strips (18 cm) over a narrower pH range (pH 4−7). For these strips, the protein concentration was approximately 0.3 mg/mL, the IPG buffer used was pH 4−7, and the volume of rehydration buffer used was 340 μL. Active rehydration of the strips was carried out at 30 V for 10 h, followed by isoelectric focusing using the following programs: (a) for 7 cm strips, 300 V "step'n hold" for 3 h, 1000 V gradient for 30 min, 5000 V gradient for 90 min, and a final focusing step at 5000 V "step'n hold" for 3 h; (b) for 18 cm strips, 500 V "step'n hold" for 1 h, 1000 V gradient for 1 h, 8000 V gradient for 3 h, 8000 V "step'n hold" for 3 h.

The focused IPG strips were then equilibrated in 2 volumes of equilibration buffer (50 mM Tris buffer, pH 8.8, containing 6 M urea, 30% w/v glycerol, 2% w/v SDS, and a trace of bromophenol blue), 10 mL containing 10 mg/mL DTT, for 15 min followed by 10 mL containing 25 mg/mL iodoacetamide for a further 15 min. The second-dimension electrophoresis was carried out either on a Bio-Rad Mini-PROTEAN 3 system for 7 cm strips or on a Bio-Rad PROTEAN II xi system for the 18 cm strips. Acrylamide gels (0.75 mm thick, 7.5% acrylamide) were cast without wells and the IPG strips laid gently on top of the gels and then sealed in place with 1% agarose. Electrophoresis was carried out at 100 V for 15 min and then increased to a constant 200 V until the end of the run. Proteins were stained using silver (*15*).

Destaining and In-Gel Tryptic Digestion of Proteins for Identification by Mass Spectrometry. The protein spots were excised from the stained gel and cut into small pieces of about 1 × 1 mm on a clean glass surface using a clean razor blade, then transferred to Eppendorf tubes, and washed with several changes of 25 mM NH_4HCO_3 followed by several changes of water. They were then suspended in 1% formic acid before being dehydrated by exposure to a solution of 50% water, 50% acetonitrile, made 1% in formic acid, for 5 min, then finally with 100% acetonitrile for 10 min. In-gel tryptic digestion was performed according to the method described by Shevchenko et al. (*17*). Briefly, the Eppendorf tubes containing the gel slices were placed in an ice−water bath, and the gel particles were allowed to swell in 25−35 μL of digestion buffer containing 12.5 ng/μL of sequencing grade trypsin in 50 mM NH_4HCO_3 for 45 min. The trypsin-containing buffer was then removed, and 5−10 μL of 50 mM NH_4HCO_3 was added to keep the pieces wet during an overnight incubation at 37 °C. After incubation, the supernatant was separated from the gel pieces by centrifugation at 11300*g* and saved in a separate Eppendorf tube; the gel pieces were re-extracted with NH_4HCO_3 (20 μL of a 20 mM solution) for 10 min, and the supernatant was pooled with that from the first extraction. The gel pieces were then re-extracted with 25 μL of 5% formic acid and 50% acetonitrile for 20 min and centrifuged at 11300*g*, and this supernatant was pooled with those from the previous steps. The formic acid extraction was repeated twice to give a final extraction volume of ∼105 μL, which was reduced using evaporation under vacuum (Savant Speed-vac, SC-100).

MALDI-TOF MS of Collagen Peptides. The rapid evaporation method was used for the sample preparation for MALDI-TOF analysis (*17*). Briefly, 1 μL of peptide matrix/nitrocellulose solution (10 mg of nitrocellulose and 40 mg of α-cyano-4-hydroxy-*trans*-cinnamic acid in 1 mL of acetone and 1 mL of isopropanol that had been freshly prepared) was applied to the sample target. Two microliters of peptide solution was then concentrated and desalted using C18 ZipTips (Millipore Corp., Bedford, MA) according to the manufacturer's instructions. One microliter of the peptide eluate from the ZipTip was then directly pipetted onto the matrix solution and the sample cocrystallized with the matrix by evaporating to dryness at ambient temperature. The organic solvent in the sample was kept below 10% to ensure that the sample solution did not completely dissolve the matrix layer. The sample target was inserted into the MALDI-TOF mass spectrometer (M@LDI Micromass) and analyzed in positive ion reflectron mode.

Immunolocation of Collagen VI. Samples of skin were cut and fixed in buffered formalin (0.0375 M phosphate buffer at pH 6.65 in 0.8% w/w formaldehyde) for 24 h before being embedded in paraffin wax. Five micrometer sections were cut from the prepared samples and floated on warm water to enable their attachment to glass slides, which were then air-dried overnight for immunocytochemical (ICC) analysis. The biotin−streptavidin detection system was used as follows: Sections were deparaffinized, then equilibrated in phosphate-buffered saline (PBS) (0.01 M phosphate NaCl 9.0 g/L), pH 7.2, for 1 min. The effect of endogenous peroxidase was mitigated by exposure to 3% hydrogen peroxide in PBS for 30 min and then equilibrated again in PBS for 1 min. A section of interest on the slide was encircled with a PAP pen (Sigma) to create a fluid barrier to hold the reagents. Nonspecific binding sites were blocked by covering the section with 1% bovine serum albumin (BSA Sigma) and allowing the slide to stand for 5 min before it was incubated in conditions of high humidity at room temperature for 1 h. The sections were then drained and washed for 1 min in each of three changes of PBS. Anticollagen VI antibodies (Chemicon AB7822 diluted 1:40 in BSA) were then added to the sections (20 μL) and again incubated at high humidity for 1 h, after which they were drained and washed in three separate changes of PBS. Approximately 100 μL of biotinylated IgG [Amersham anti-rabbit from sheep (RPN1004) diluted 1:200 in BSA] was added, and the sections were incubated as previously for 30 min. They were then drained and washed in three changes of PBS before being exposed to a preformed

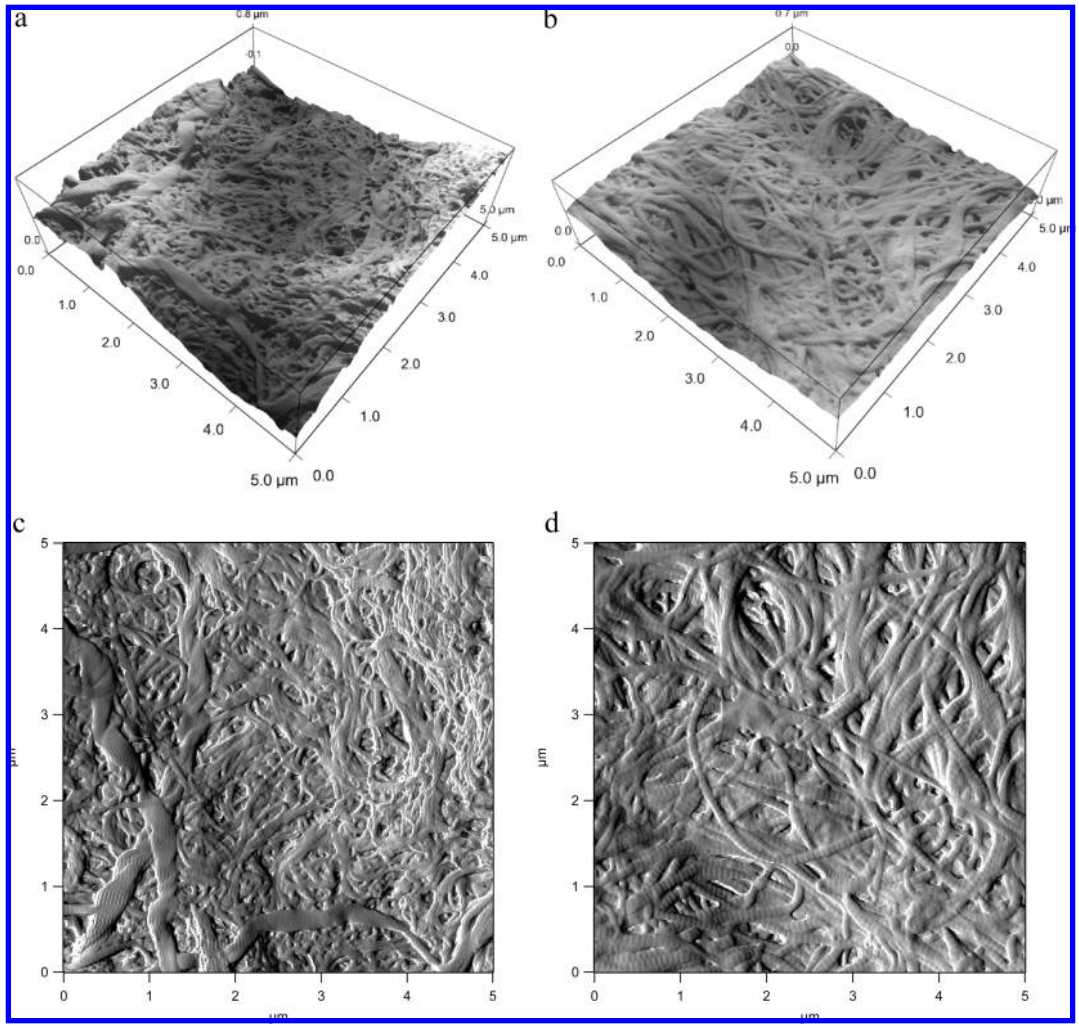

Figure 2. AFM images of the outermost surface of conventionally and enzymatically depilated pickled lambskin scanned at 20 μm resolution: (**a**, **c**) conventionally depilated skin showing the fine mesh of collagen fibrils; (**b**, **d**) outermost surface of enzymatically depilated pickled lambskin. Much of the collagen is visible as single fibrils. Some fibrils lie enmeshed with others, but a significant number appear loose and independent of the rest of the surface structure.

biotin−streptavidin−peroxidase complex (streptavidin−biotinylated horseradish peroxidase RPN1051 diluted 1:200 in BSA). Sections were then drained and washed in three changes of PBS before flooding with 10 mL of 0.5 mg/mL 3,3-diaminobenzidine (DAB), containing 20 μL of 30% peroxide for approximately 3 min. The color was allowed to develop for approximately 3 m before the reaction was halted by immersion of the sections in PBS. The sections were rinsed in tap water before being counterstained with Mayer's hämalaun for 1 min, after which they were rinsed in tap water, dehydrated, cleared, and mounted in DPX mounting medium. The sections were examined under a light microscope at 40× magnification, where collagen VI was visualized as a brown/black stain.

RESULTS AND DISCUSSION

Damage to the surface of leather as a result of enzymatic depilation is the major reason the technology has not been generally adopted. Thus, although it would be very desirable to develop a process that uses only enzymes for environmental reasons, one has to be developed that does not compromise the integrity and desirable characteristics of the leather. A first step toward developing a commercially viable process is to identify the macromolecules present in good-quality leather and then to compare them to those present in an inferior product. Such knowledge will allow enzymes and processes to be selected that do not damage molecules found to be present in quality products. In this work we have attempted to analyze the protein constituents and structure of the enamel, the most important part of the skin as far as its appearance is concerned, to determine whether the removal of specific proteins is responsible for the differences observed in the products from conventionally processed and enzymatically depilated skins.

Using atomic force microscopy it was possible to view the differences in the surfaces of the two halves of the skin that had been processed using either enzymes or the conventional sulfide-based process. The enamel layers of a conventionally processed and an enzyme-depilated sample are shown in **Figure 2a**,**b** and **Figure 2c**,**d**, respectively, where differences in their surface topographies are clearly evident. The enamel layer of the conventionally treated material shows a fine, tightly interwoven mesh of individual collagen fibrils lying at different angles to one another (**Figure 2a**,**b**). In contrast, the individual fibers at the surface of the enzyme-depilated material (**Figure 2c**,**d**) appear to be disentangled from that fine mesh and the weave of the mesh appears to be much looser and more open than the conventionally treated material.

The finding that disruption of the fine mesh of individual collagen fibrils results from enzyme depilation is novel; it could potentially allow easier access of reagents to the skin proteins during processing, making the skin more sensitive to chemical

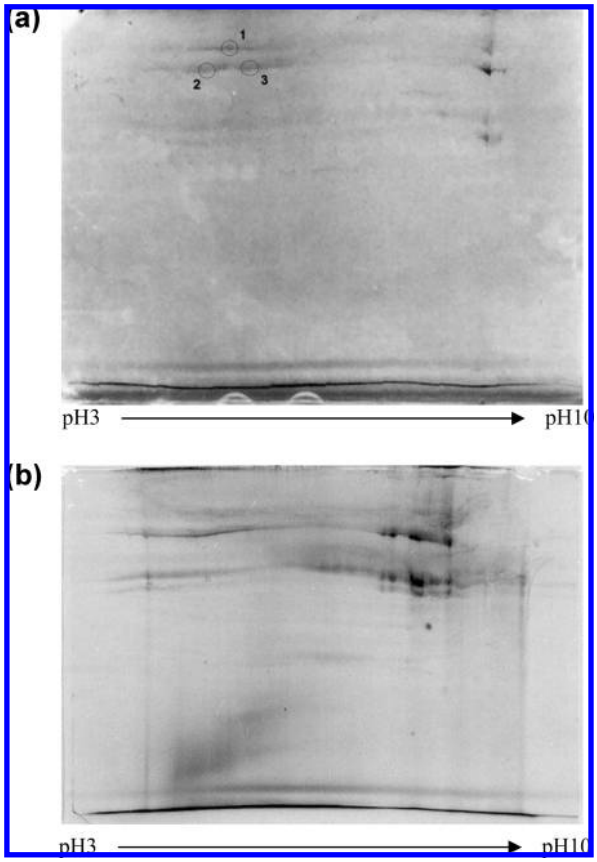

Figure 3. (**a**) 2D electrophoretic (8 × 10 cm) pattern of the sample sectioned from the enamel layer of the conventionally depilated skin. Note the spot labeled 1, which was not identified in material sectioned from the remainder of the grain layer, indicating it is a protein that is relatively rich in the enamel layer. Spots 2 and 3 represent other proteins that are present in the enamel layer as well as in the remainder of the grain layers. (**b**) 2D electrophoretic (8 × 10 cm) pattern of the sample sectioned from the region of the grain underneath the enamel layer of the conventionally depilated skin. Note the absence of a spot in the location of spot 1 from panel **a**.

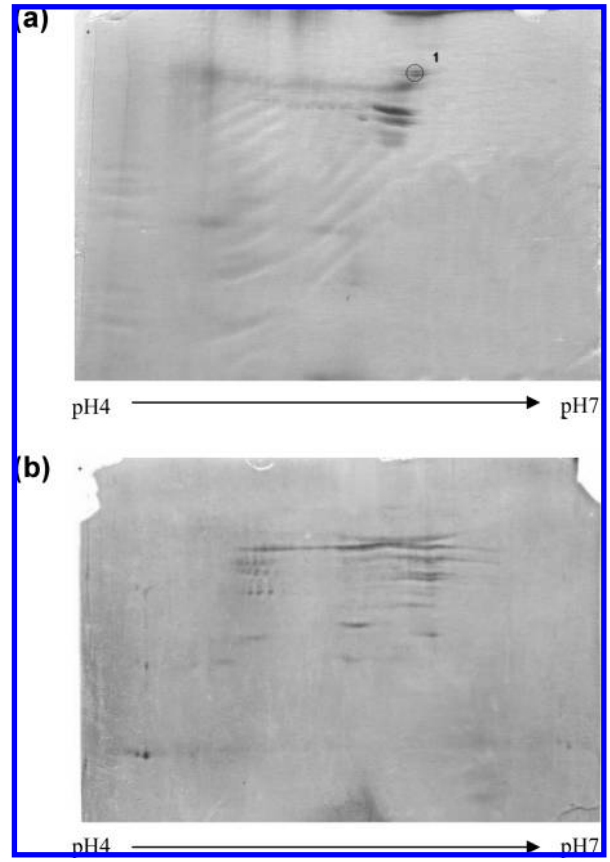

Figure 4. (**a**) 2D electrophoretic (18 × 20 cm) pattern of the sample sectioned from the enamel layer of the conventionally depilated skin. Note that the spot labeled 1, which does not appear in other samples, is split, possibly due to cleavage of the peptide or the partial removal of glycosaminoglycans. The entire spot was sampled for MALDI-TOF analysis. (**b**) 2D electrophoretic (18 × 20 cm) pattern of the sample sectioned from the enamel layer of the enzymatically depilated skin. Note the absence of a spot in the location of spot 1 from panel **a**. Also note the large number of proteins present in the enzyme-depilated skin extract in comparison to the conventionally depilated skin.

damage, especially alkali damage because of the high pH of the solutions used. Such a change in structure at the microscopic level could ultimately manifest itself as a weakening and dulling of the grain enamel so often observed at the macroscale after enzyme processing. If this is true, it follows that the event that causes the release of fibrils in the grain enamel is the underlying cause of the grain damage observed when skins are depilated using enzymes and implies that some sort of structure or molecule that binds the collagen fibrils into a tightly woven mesh may be removed during processing. This finding supports an earlier work which showed that enzyme treatment of pig skin caused a weakening of the affinity between fibrils, which led in turn to a separation of fibrils (*3*).

To further investigate the damage caused by enzymatic depilation of skin, 2D gel electrophoresis was carried out to analyze the proteins both in the enamel and within the remainder of the grain layer to identify any important differences in the protein complement of the skins using peptide mapping. The 2D electrophoretic pattern of proteins comprising both the enamel layer and the remainder of the grain layer exposed after removal of the enamel layer from both conventionally (**Figures 3a**,**b** and **4a**) and enzymatically (**Figure 4b**) pickled skin extracts showed that, as has been previously reported, the majority of them focused between pH 5 and 6 (*9*).

Enrichment of the proteins in the enamel layer by selective microtome sectioning resulted in different electrophoretic patterns as can be seen in **Figure 3a**,**b**. The most abundant proteins in the enamel layer of conventionally depilated skin, spots 1−3 (**Figure 3a**), were analyzed further. It is worth noting that spot 1 did not appear in the 2D gel of the section immediately below the enamel layer of the conventionally depilated skin (**Figure 3b**), indicating that careful sectioning is able to differentiate the protein complement of the different layers of the skin.

To identify proteins lost or modified during enzymatic dewooling, spots 1−3 (**Figure 3a**) were excised from the 2D gel of the conventionally processed enamel layer, and tryptic peptides were generated from each spot. The samples were subjected to MALDI-TOF MS and proteins identified using the monoisotopic masses of the peaks generated from each spot (MASCOT, Matrix Science). The search parameters allowed for one missed cleavage, carbamidomethylation of cysteine residues, and possible oxidation of methionine residues. The peptide tolerance for the experimental peptide mass value was set at ±1 Da, and peptides from individual spots were matched with the monoisotopic masses of peptides from mammalian proteins. Sequences were also compared to those from bovine and human skin proteins as there is a shortage of protein sequence data from sheep proteins in the publicly accessible databases. Comparisons with bovine proteins have previously

Table 1. Proteins Identified from Spots in 2D Gel Electrophoresis

spot	Figure	Table	protein name	source	UniProtKB/TrEMBL entry name
1	3a	2a	collagen, type VI, α 2	*Bos taurus*	Q1JQB0_BOVIN
1	3a	2b	collagen, type VI, α 3 [fragment]	*Ovis aries*	Q9MZW2_SHEEP
2	3a	3	collagen, type III, α 1	*Bos taurus*	CO3A1_BOVIN[a]
1	4a	4a	collagen, type VI, α 2	*Bos taurus*	Q1JQB0_BOVIN
1	4a	4b	collagen, type VI, α 3 [fragment]	*Ovis aries*	Q9MZW2_SHEEP
1	4a	4c	collagen, type VI, α 2 [precursor]	*Homo sapiens*	CO6A2_HUMAN

[a] Originally referenced as PIR-PSD entry CGBO7S.

Table 2. Observed and Calculated Masses of the Tryptic Peptides from Spot 1 Derived from **Figure 3a**

exptl *m*/*z* transformed to a rel mol mass	calcd rel mol mass	missed cleavage	position of matched peptides
(**a**) As Matched with UniProtKB/TrEMBL Entry Name Q1JQB0_BOVIN[a]			
1180.593	1179.636	1	$S^{120}-R^{129}$
615.3927	615.334	0	$L^{174}-R^{178}$
602.2427	602.3024	0	$E^{181}-R^{185}$
587.2027	587.3391	1	$G^{264}-K^{269}$
1198.663	1199.524	0	$G^{270}-K^{281}$
807.3927	807.3511	0	$G^{309}-R^{316}$
669.3127	669.381	0	$G^{318}-K^{325}$
530.1927	529.3336	1	$G^{333}-R^{337}$
1328.663	1328.614	1	$I^{338}-R^{350}$
591.1327	590.266	0	$G^{366}-K^{371}$
825.1427	825.3981	0	$G^{381}-K^{389}$
796.3627	796.4191	1	$G^{417}-R^{424}$
574.2127	573.2758	0	$G^{426}-K^{431}$
1324.643	1325.621	1	$G^{426}-K^{440}$
1194.583	1194.563	1	$G^{441}-R^{452}$
1706.743	1705.838	1	$G^{444}-K^{461}$
923.4727	923.4937	1	$G^{465}-R^{473}$
840.4027	840.3726	0	$G^{489}-R^{497}$
841.4027	841.393	0	$G^{498}-K^{506}$
544.1927	543.2653	0	$G^{521}-K^{526}$
514.3127	514.25	0	$G^{545}-R^{549}$
572.2527	571.3693	0	$L^{644}-K^{649}$
988.5527	989.4778	1	$D^{650}-R^{658}$
896.4227	895.4651	0	$I^{680}-K^{687}$
745.3727	744.4494	1	$L^{713}-R^{718}$
1365.623	1364.643	1	$H^{734}-R^{744}$
1366.633	1366.68	0	$N^{784}-K^{795}$
1383.663	1382.675	0	$N^{784}-K^{795}$
1232.583	1232.567	0	$T^{835}-R^{845}$
1233.653	1232.713	0	$L^{869}-R^{879}$
524.1527	523.3231	0	$L^{901}-R^{904}$
(**b**) As Matched with UniProtKB/TrEMBL Entry Name Q9MZW2_SHEEP[b]			
574.2127	573.3486	0	$V^{1}-K^{6}$
1717.793	1717.9	1	$V^{25}-K^{40}$
988.5527	989.4665	0	$N^{32}-K^{40}$
1037.523	1036.53	0	$I^{41}-R^{50}$
533.1627	532.2857	0	$G^{109}-K^{113}$
1302.663	1303.655	0	$I^{127}-R^{138}$

[a] Mass, 98215; score, 213; expect, 3.4E−16; queries matched, 31; coverage, 26%. [b] Mass, 98215; score, 80; expect, 0.0075; queries matched, 6; coverage, 19%.

been reported on the assumption that only a few homologous peptide sequences are required for a successful match (*18*).

Spot 1, which was absent from the 2D gel profiles generated from the grain layer of the conventionally treated skins, showed good correlation with peptides from collagen type VI of both bovine and ovine skin (**Tables 1**, and **2a**,**b**), indicating significant homology between collagens from these two species. Spots 2 and 3 appeared in the gels of both the enamel and grain layers (panels **a** and **b**, respectively, of **Figure 3**), and spot 2 was identified as type III collagen (**Tables 1** and **3**).

To confirm these results, and more specifically the presence or absence of collagen VI in the enamel layers of conventionally

Table 3. Observed and Calculated Masses of the Tryptic Peptides from Spot 2 Derived from **Figure 3a** As Matched with UniProtKB/TrEMBL Entry Name CO3A1_BOVIN[a]

exptl *m*/*z* transformed to a rel mol mass	calcd rel mol mass	missed cleavage	position of matched peptides
1648.851	1648.851	1	$G^{153}-R^{170}$
2054.029	2054.029	1	$G^{258}-K^{280}$
1707.781	1707.781	0	$D^{311}-R^{329}$
631.3441	631.3442	0	$G^{330}-R^{335}$
764.3929	764.3929	0	$G^{354}-R^{362}$
1320.679	1320.679	0	$G^{624}-R^{638}$
2719.831	2719.331	1	$G^{672}-K^{704}$
839.4501	839.4501	0	$G^{813}-K^{821}$
948.5028	948.5029	0	$G^{984}-K^{994}$

[a] Mass, 93708; score, 78; expect, 0.01; queries matched, 9; coverage, 13%.

and enzymatically depilated skins, large-format 2D gel electrophoresis was carried out over a narrower pH range (pH 4−7) (**Figure 4a**,**b**). Again, the major difference between the 2D patterns of the enamel layers was the absence of a significant number of proteins from the conventionally depilated material that were present in the enzymatically depilated material. A glaring exception to this trend was the absence in **Figure 4b** of a spot in the same position as spot 1 in **Figure 4a**. This was again identified as collagen VI (**Table 4**) on the basis of the significant sequence homologies between the fragments of translated nucleotide sequence from sheep collagen VI and the translated nucleotide sequences of bovine and human collagen VI as determined by the sequence alignment tool Clustal W (*19*). The results obtained from the small-format gels were thus confirmed. This finding is both novel and original and may have important implications for the integrity of enzyme-depilated skins.

Immunolocalization studies were carried out to validate the presence of collagen VI in the enamel. It was found that ovine collagen VI was recognized by polyclonal antibodies to human collagen VI (**Figure 5a**), which allowed the location of this particular collagen in the different skin sections to be established. Collagen VI was found throughout the enamel, particularly in the region immediately below the epidermal cells. Conventional processing did not remove the collagen VI from this region (**Figure 5b**) in contrast to the enzyme-depilated material, which showed no significant staining (**Figure 5c**).

The fiber-forming collagens present in skin are mainly types I and III and perhaps to a lesser extent type V. Any of these types can form fibrils in combination with each other or on their own. Type I and III collagens, in particular, have been shown to resist liming, bating, and pickling (*20, 21*).

Collagen VI, however, has been shown to react differently to proteolytic attack; it has been shown to be resistant to collagenase under nonreducing conditions in contrast to collagens I−V, implying that there are differences in its structure (*22*). It is therefore not surprising that it confers specific properties to the tissue in which it is found.

Previous immunolocalization studies showed that collagen VI microfibrils form extensive filamentous networks intercalated between interstitial collagen I and II fibrils (*23–25*), where they act to anchor them to the basement membranes (*26*). Collagen VI monomers consist of a short triple-helical domain with a large globular domain at each end (*27*) and have been shown to assemble intracellularly into dimers and tetramers (*28*). These are then secreted into the extracellular matrix, where they assemble into microfibrillar structures by end-to-end association (*28*). The structural features of collagen VI, along with its Arg−Gly−Asp cell binding sequences in the triple-helical

Table 4. Observed and Calculated Masses of the Tryptic Peptides from Spot 1 Derived from **Figure 4a**

exptl *m/z* transformed to a rel mol mass	calcd rel mol mass	missed cleavage	position of matched peptides
(**a**) As Matched with UniProtKB/TrEMBL Entry Name Q1JQB0_BOVIN[a]			
2705.159	2704.412	1	$H^{147}-K^{173}$
614.3877	615.334	0	$L^{174}-R^{178}$
1350.663	1349.701	0	$V^{248}-K^{260}$
2150.967	2150.116	1	$Q^{284}-K^{305}$
806.4067	807.3511	0	$G^{309}-R^{316}$
1054.517	1053.575	1	$L^{335}-K^{344}$
981.4637	981.4992	1	$R^{380}-K^{389}$
1193.585	1194.563	1	$G^{441}-R^{452}$
840.3997	840.3726	0	$G^{489}-R^{497}$
543.1727	543.2653	0	$G^{521}-K^{526}$
514.3157	514.25	0	$G^{545}-R^{549}$
988.5607	989.4778	1	$D^{650}-R^{658}$
896.4307	895.4651	0	$I^{680}-K^{687}$
2367.192	2366.206	1	$N^{692}-K^{712}$
744.3877	744.4494	1	$L^{713}-R^{718}$
1364.633	1364.643	1	$H^{734}-R^{744}$
1233.656	1232.713	0	$L^{869}-R^{879}$
2064.035	2063.03	1	$Q^{889}-R^{904}$
(**b**) As matched with UniProtKB/TrEMBL Entry Name Q9MZW2_SHEEP[b]			
988.56	989.466	0	$N^{32}-K^{40}$
1035.532	1036.53	0	$I^{41}-R^{50}$
1649.769	1650.751	0	$A^{7}-R^{21}$
2007.896	2007.985	1	$N^{32}-R^{50}$
2565.162	2565.263	1	$A^{86}-K^{108}$
(**c**) As Matched with UniProtKB/TrEMBL Entry Name CO6A2_HUMAN[c]			
1340.0117	1339.681	0	$V^{4}-K^{16}$
1715.8157	1715.867	1	$V^{4}-R^{19}$
2150.9667	2150.116	1	$Q^{40}-K^{61}$
806.4067	807.3511	0	$G^{65}-R^{72}$
1054.5167	1053.575	1	$L^{91}-K^{100}$
614.3877	614.2772	0	$G^{101}-R^{106}$
2039.9527	2040.889	1	$G^{101}-R^{121}$
1987.8557	1986.867	1	$G^{107}-K^{127}$
981.4637	980.5403	1	$R^{136}-K^{145}$
824.1607	824.4392	0	$G^{137}-K^{145}$
1193.5847	1194.563	1	$G^{197}-R^{208}$
1587.6947	1586.853	1	$G^{224}-K^{240}$
1437.7197	1437.732	1	$G^{230}-R^{244}$
840.3997	840.3726	0	$G^{245}-R^{253}$
1164.5827	1164.564	1	$G^{283}-R^{294}$

[a] Mass, 98215; score, 133; expect, 3.4E−08; queries matched, 17; coverage, 21%. [b] Mass, 27076; score, 72; expect, 0.047; queries matched, 5; coverage, 23%. [c] Mass, 33294; score, 183; expect, 3.4E−13; queries matched, 15; coverage, 42%.

domain, make it ideally suited to playing a role in cell−matrix and matrix−matrix association (*29*). Furthermore, "Von Willebrand factor A" domains (specific collagen-binding domains) in collagen VI are not only thought to be involved in self-interactions but also appear to be involved in binding to fibrillar proteins such as collagen type I (*30*).

The presence of collagen VI in the grain enamel layer, which persists even after conventional processing up to the pickled pelt stage, was reported earlier (*31*) and has been confirmed by the immunolocalization studies in this work. The presence of nonfibrillar collagens such as collagen VI has been shown to be concentrated on the surface of the fibrils, probably enhancing the tendency of the fibers and fibrils to be very tightly associated with each other (*20*).

This work therefore confirms other reports' positioning collagen VI in the grain enamel and also shows that collagen VI is removed from the surface collagen fibrils during enzymatic depilation. Due to its association with collagen type I fibrils, and its function of binding them together, the removal of collagen VI might result in the loosening of fibril mesh at the skin surface as observed (**Figure 2c**,**d**). It is therefore possible that the removal of collagen VI through enzymatic depilation could cause a reduction in the structural stability of the fibrillar

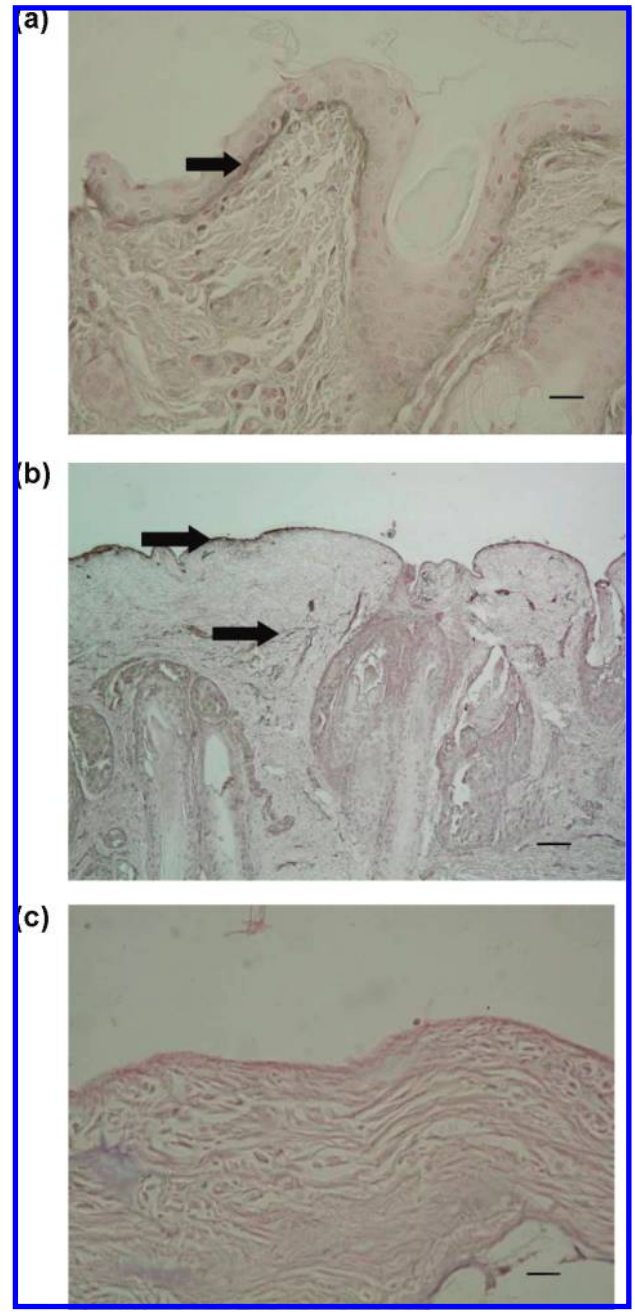

Figure 5. (**a**) Immunolocalization of collagen VI from raw skin. Collagen VI is clearly visible as the darker brown area below the level of the epidermal cells at the top of the dermal region as indicated by the arrow. The bar is 25 μm. (**b**) Conventionally processed skin collagen VI immunolocalization. Collagen VI is visible at the top of the dermal region (found at the top of the section because the epidermal cells have been removed) and within the bottom of the enamel layer as indicated by the arrows. The bar is 25 μm. (**c**) Enzymatically processed skin collagen VI immunolocalization. After enzyme processing the collagen VI that was visible within the raw skin at the dermal surface is no longer visible in any significant quantity. The bar is 25 μm.

arrangement at the skin surface. Removal of collagen VI from the enamel layer of the skin is consistent with a deterioration of the fine structure at the skin surface and may be the underlying cause of the damage observed to occur to the surface of enzymatically depilated skins. This knowledge will assist in the development of enzymatic processing regimens that do not remove collagen VI and is a step toward to an entirely enzyme-based process that is acceptable to the leather industry.

LITERATURE CITED

(1) Sivasubramanian, S.; Murali Manohar, B.; Puvanakrishnan, R. Mechanism of enzymatic dehairing of skins using a bacterial alkaline protease. *Chemosphere* **2008**, *70*, 1025–1034.

(2) Cantera, C. S.; Garro, M. L.; Goya, L.; Barbeito, C.; Galarza, B. The diffusion barrier within the unhairing process. *World Leather* **2005**, *18* (6), 29–32.

(3) Wang, Y.; Li, Z.; Chen, M.; Cheng, H.; Liao, L. Study on changes of collagen fibril structure in pigskin tissue after enzyme treatment. *J. Soc. Leather Technol. Chem.* **2005**, *89* (2), 47–56.

(4) He, Q.; Yao, K.; Sun, D.; Shi, B. Biodegradability of wastewater from enzymatic soaking and unhairing processes in leather manufacture. *J. Am. Leather Chem. Assoc.* **2006**, *101*, 217–222.

(5) Gehring, A. G.; DiMaio, G. L.; Marmer, W. N.; Mazenko, C. E. Unhairing with proteolytic enzymes derived from *Streptomyces griseus*. *J. Am. Leather Chem. Assoc.* **2002**, *97* (10), 406–411.

(6) Keller, W. The quantitative composition of the skin papillary layer and its transformation in the beamhouse processes. *Leder Haeutemarkt, Gerbereiwissenschaft Praxis* **1990**, *42*, 117–127.

(7) Alexander, K. T. W.; Haines, B. M.; Walker, M. P. Influence of proteoglycan removal on opening up in the beamhouse. *J. Am. Leather Chem. Assoc.* **1986**, *81*, 85–102.

(8) Stirtz, T. Processes in the skin under the influence of bating enzymes Part 2. Changes in the hide substance through bating proteases with special emphasis on leather-forming collagen. *Das Leder* **1982**, *33*, 67–78.

(9) Deb Choudhury, S.; Allsop, T.; Passman, A.; Norris, G. E. Use of a proteomics approach to identify favourable conditions for production of good quality lambskin leather. *Anal. Bioanal. Chem.* **2006**, *384*, 723–735.

(10) Germann, H. P. The evolution of the unhairing process as influenced by technological, economic and ecological considerations. *J. Am. Leather Chem. Assoc.* **1997**, *92* (4), 84–92.

(11) Dempsey, M. *Hide, Skin and Leather Defects: A Guide to Their Microscopy*; New Zealand Leather and Shoe Association: Palmerston North, New Zealand, 1984.

(12) Haines, B. M. Twentieth Procter memorial lecture: the skin before tannage—Procter's view and now. *J. Soc. Leather Technol. Chem.* **1984**, *68*, 57–70.

(13) Bienkiewicz, K. *Physical Chemistry of Leather Making*; Robert, E., Ed.; Kreiger Publishing: Malabar, FL, 1983.

(14) Stewart, K. J. A quantitative ultrastructural study of collagen fibrils in human skin normal scars, and hypertrophic scars. *Clin. Anat.* **1995**, *8* (5), 334–338.

(15) Berkelman, T.; Stenstedt, T. 2-D Electrophoresis, Using Immobilized PH Gradients, Principles and Methods; Amersham Biosciences; 80-6429-60 Rev-A, 10/98, 1998.

(16) Bradford, M. M. A rapid and sensitive method for the quantitation of microgram quantities of protein utilizing the principle of protein-dye binding. *Anal. Biochem.* **1976**, *72*, 248–254.

(17) Shevchenko, A.; Wilm, M.; Vorm, O.; Mann, M. Mass spectrometric sequencing of protein from silver-stained polyacrylamide gels. *Anal. Chem.* 199668, 850–858.

(18) Simpson, D. M.; Beyon, R. J.; Robertson, D. H. L.; Loughran, M. J.; Haywood, S. Copper associated liver discease: A proteomics study of copper challenge in a sheep model. *Proteomics* **2004**, *4*, 524–536.

(19) Chenna, R.; Sugawara, H.; Koike, T.; Lopez, R.; Gibson, T. J.; Higgins, D. G.; Thompson, J. D. Multiple sequence alignment with the Clustal series of programs. *Nucleic Acids Res.* **2003**, *31*, 3497–3500.

(20) Kronick, P. L.; Iandola, S. Persistence of minority macromolecules of hide through the beamhouse. II. Removal of collagen type XIV. *J. Am. Leather Chem. Assoc.* **1997**, *92*, 172–178.

(21) Kronick, P. L., III. Persistence of decorin. *J. Am. Leather Chem. Assoc.* **1998**, *93*, 148–155.

(22) Heller-Harrison, R. A.; Carter, W. G. Pepsin generated type VI collagen is a degradation product of GP140. *J. Biol. Chem.* **1984**, *259* (11), 6858–6864.

(23) Kuo, H. J.; Maslen, C. L.; Keene, D. R.; Glanville, R. W. Type VI collagen anchors endothelial basement membranes by interacting with type IV collagen. *J. Biol. Chem.* **1997**, *272*, 26522–26529.

(24) Cay, M.; Kielty, C.; Shuttleworth, A. Microfibrillar elements of the dermal matrix. *Microsc. Res. Tech.* **1997**, *38* (4), 413–427.

(25) Keene, D. R.; Ridgway, C. C.; Iozzo, R. V. Type VI microfilaments interact with a specific region of banded collagen fibrils in skin. *J. Histochem. Cytochem.* **1998**, *46*, 215–220.

(26) Zeichen, J.; van Griensven, M.; Albers, I.; Lobenhoffer, P.; Bosch, U. Immunohistochemical localization of collagen VI in arthrofibrosis. *Arch. Orthopaedic Trauma Surg.* **1999**, *119*, 5–6.

(27) Chu, M.; Pan, T.; Conway, D.; Saitta, B.; Stokes, D.; Kuo, H.; Glanville, R. W.; Timpl, R.; Man, K.; Deutzmann, R. *Structure, Molecular Biology, and Pathology of Collagen*; Fleischmajer, R., Olsen, B. R., Kühn, K., Eds.; New York Academy of Sciences: New York, 1990; Vol. 580.

(28) Engvall, E.; Hessle, H.; Klier, G. Molecular assembly, secretion, and matrix deposition of type VI collagen. *J. Cell Biol.* **1986**, *102*, 703–710.

(29) Aumailley, M.; Speks, U.; Timpl, R. Cell adhesion to type VI collagen. *Biochem. Soc. Trans.* **1991**, *19*, 843–847.

(30) Veit, G.; Kobbe, B.; Keene, D. R.; Paulsson, M.; Koch, M.; Wagener, R. Collagen XXVIII, a novel von Willebrand Factor A domain-containing protein with many imperfections in the collagenous domain interacts with avian Tenascin-X through its NC3 domain. *J. Biol. Chem.* **2006**, *281* (6), 3494–3504.

(31) Kronick, P. L.; Maleeff, B. E.; Dahms, M. P. Removal of collagens VI and XII by beamhouse chemistry. *J. Am. Leather Chem. Assoc.* **1991**, *86* (6), 209–224.

Received for review February 7, 2008. Revised manuscript received June 24, 2008. Accepted June 24, 2008.

JF800380Y